CIRP Annals - Manufacturing Technology 62 (2013) 63–66

Contents lists available at SciVerse ScienceDirect

CIRP Annals - Manufacturing Technology

journal homepage: http://ees.elsevier.com/cirp/default.asp

Nanostructural evolution of hard turning layers in response to insert geometry, cutting parameters and material microstructure

V. Bedekar [a,b], R. Shivpuri (1)[b,*], R. Chaudhari [a], R. Scott Hyde [a]

[a] Timken Technology Center, N. Canton, OH 44720, USA
[b] Department of Integrated Systems Engineering, The Ohio State University, Columbus, OH 43210, USA

ARTICLE INFO

Keywords:
Hard machining
White layer
Nano structure

ABSTRACT

Nanostructural characterization of hard turned surface layers of carburized steels was done to study the effect of tool design, tool wear and turning parameters on the near surface material transformations. To quantify subsurface evolution, numerical predictions were correlated with the measured structural and hardness parameters. Results show that the process design space can be partitioned into three regions based on thermal phase transformations, plastic grain refinement, and where both mechanisms are active. These relationships between the processing conditions and structural parameters are further explored through process maps based on Zener–Holloman parameter and the Hall–Petch relationship.

1. Introduction

The primary objective of hard turning is to produce surfaces with high dimensional accuracy and surface integrity that enhance functional performance. In a detailed empirical study, Tonshoff et al. [1] studied the effects of insert geometry on cutting forces and the effects of insert wear on white layer and surface integrity. A few TEM (transmission electron microscopy) investigations [2–4] have shown that white layers are comprised of subgrains with size in the range of 30–100 nm. Akcan et al. [4] suggested that the white layers are formed due to high strains and discussed dynamic recrystallization. Most of these investigations focus on a thermally induced white layer formed by reverse martensitic transformation. Their conclusions are supported by an increase in the retained austenite (RA) content at higher cutting temperatures. However, traditional X-ray diffraction (XRD) analysis has limited use in this application since the X-ray penetration depths are in the range of 5–10 μm depending upon angle of incidence, compared with depths of white layers which could be as shallow as 1–2 μm. Recently, Hosseini et al. [5] conducted glancing angle XRD (GAXRD) to analyze the %RA transformation and found that depending upon cutting conditions, the white layer could be plastically or thermally induced. Jawahir et al. [6] called for use of advanced characterization techniques to understand the structure and morphology of white layer. Traditional techniques such as scanning electron microscopy, optical microscopy and XRD are limited in their ability to reveal structures that are as small as few tens of nanometers, and are shallower than 1 μm. Also, carburized steel has received little attention in hard turning studies.

This study interrogates the process–structure relationship in hard turning by exploiting recent advances in microstructural characterization techniques, especially the role of thermomechanical phenomena in nanostructural changes and phase transformations in hard turned surfaces. A goal being the use this knowledge in the design of machining processes for the desired structural, hardness and residual stress states that can be used for improvements in the life cycle of a machined component.

2. Experimental

Hard turning experiments were conducted on carburized SAE 8620 steel with 30% retained austenite. Rings of 285 mm outer diameter, 245 mm inner diameter and 38 mm width were carburized and hardened. Hardening was performed at 885 °C for 2 h to dissolve most of the primary carbides and to retain maximum carbon in solution. Subsequent tempering was performed for 2 h at 180 °C. Vickers microhardness testing indicated that hardness values ranged from 60.1 to 61.7 HRc to depths up to 1.524 mm. Retained austenite content was confirmed using traditional and GAXRD.

Hard turning was performed on a high precision horizontal CNC lathe. Two insert geometries with varying rake angles and different levels of cutting speeds and insert wear conditions were used to produce white layers with different microstructures (Table 1). The insert geometries were chosen to impart distinct microstructural alterations. Upsharp positive rake inserts (UP) were designed in such a way that they could be placed in the same tool holder as the honed negative rake (NH) inserts. Low PCBN insert tips with DNGA431 geometry were used. Cutting was performed using a soluble oil based coolant. All experiments utilized a constant depth of cut (100 μm) and feed rate (50 μm). Insert wear was limited to 100 μm to ensure low surface roughness.

Table 1
Experimental conditions or hard turning.

Insert geometry	−20° rake and 50 μm hone (NH), +5° rake and 12 μm hone (UP)
Cutting speed	91 m/min, 273 m/min
Flank wear (VB)	0 μm (F-fresh), 100 μm (W-worn)
Nomenclature	*Negative Rake Worn Insert = NH-W and so on.*

* Corresponding author.

0007-8506/$ – see front matter © 2013 CIRP.
http://dx.doi.org/10.1016/j.cirp.2013.03.090

Cross sectional TEM samples were prepared using the Helios Dual Beam Focused Ion Beam (FIB) Mill with a Gallium liquid metal source. The site of interest was coated with platinum using an electron beam, and low voltage (5 kV) to preserve the surface. The final dimensions of the FIB samples were approximately 10 μm × 10 μm × 100 nm. A FEI Tecnai F30 TEM was used for the analyses. The camera factor was established using a standard silicon sample with a *d*-spacing of 3.14 Å. Dark field imaging was performed using beam tilt to minimize spherical aberration.

GAXRD was performed to characterize changes in retained austenite at very shallow depths. Analyses were performed using a prototype diffractometer at Proto Inc. using a Cu-Kα source. To reduce fluorescent radiation, the machine was equipped with Cd-Te detector with 200 eV FWHM that cleanly separates CuKα from FeKα. Additionally, the detector side soller slits were used. The tests were conducted using 28 kW power and 17 mA current; with a time step of 60 s and step increments of 0.1°. The study utilized customized curve fitting software with split Pearson 7. The scan was performed to include $\{2\,0\,0\}_\gamma$, $\{2\,2\,0\}_\gamma$, $\{1\,1\,0\}_\alpha$ and $\{2\,0\,0\}_\alpha$ $h\,k\,l$ planes. Retained austenite calculations were performed using the technique detailed by Jatczak et al. [7]. An incident angle of 3° allowed penetration depths as shallow as 150-300 nm.

To characterize the nanohardness, nanoindentation tests were conducted at Nanomechanics Inc using Agilent Technologies Nanoindentor G200 with an Express Test option [8]. The samples were coated with chromium to preserve the edge and a 10 μm × 10 μm area was indented using a 30 × 30 array of 900 indentations. A Berkovich indentor was used with an applied force of 1.5 mN at a depth of 82 nm. Area calibrations were performed on fused silica and indent spacing was determined by conducting consecutive arrays of indents with decreasing separation distance until errors were generated in the hardness measurements; a minimum spacing of 3.5 times the maximum depth was empirically determined.

Plane strain numerical modeling of turning was performed using DEFORM 2D® V10.2 software. A rigid-plastic model was used with hardness based flow stress model [9]. Brozzo's fracture criterion was utilized for chip separation, and the model was validated by the force data available in the literature [10].

3. Results

3.1. Transmission electron microscopy

The bright field (Fig. 1) and dark field (Fig. 2) TEM images revealed that regardless of speed and insert conditions, all samples exhibited a severely transformed layer with a depth in the range of 400–600 nm with a new insert, and 1000–1400 nm with a worn insert. The surfaces machined with either UP (refer Table 1 for insert description) inserts or lower cutting speed indicated slightly shallower deformation depths. It is interesting to note that the optical microscopy did not reliably reveal the deformation layers except when the depth of deformation was in the range of 900–1400 nm. The bright field images at lower cutting speed (Fig. 1a and b) indicated transformation of martensite laths into rounded nanograins, while the higher cutting speed image showed partial dissolution of carbides (Fig. 1c). Since dark field imaging provides better contrast of grains in diffracting condition, it was used to analyze the sub-grain size. Fig. 2 shows the dark field images of the near surface sub-grain evolution of the surface machined with an NH insert. The micrographs showed that the deformation layers exhibited equiaxed nanocrystalline grains of varying sizes. The grains were misoriented with a size range that was about 100 times smaller than the grain size of the base microstructure (2 μm). The surface machined with NH-F at 91 m/min showed mean sub grain size of approximately 20 nm (Fig. 2a). The subgrain size

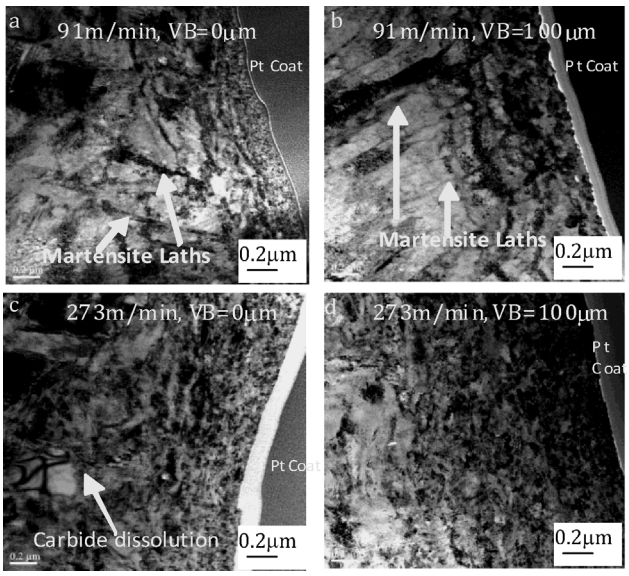

Fig. 1. Bright field TEM images of hard turned surface using UP insert at 17.5 kX.

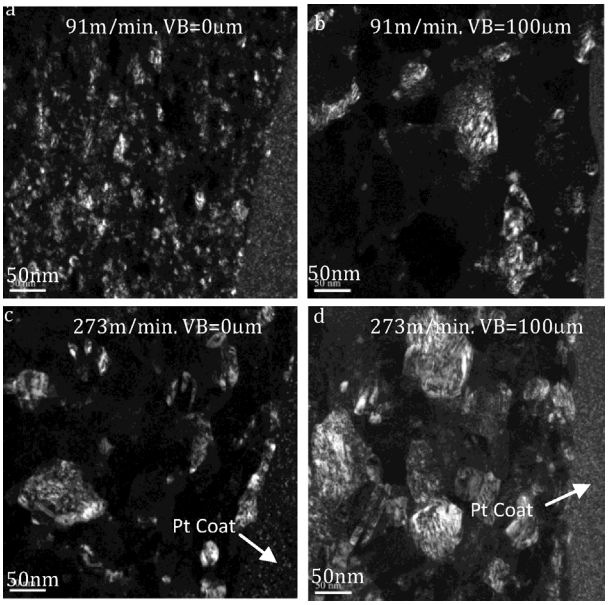

Fig. 2. Dark field TEM images of hard turned surface using NH insert at 63 kX.

increased gradually as the insert wore (Fig. 2b and d), but significant grain coarsening was observed when the speed was increased from 91 m/min to 273 m/min (Fig. 2a and c).

The increase in the grain size with insert wear is mainly due to dynamic recrystallization caused by the grain boundary annihilation; however it must be assisted by a slight increase in the temperature due to higher friction between the workpiece and worn tool. On the contrary, the increase in grain size at higher cutting speed is mainly due to the higher temperature generated at the tool workpiece interface. To assess the significance of process parameters to the measured characteristic, the Student's *t*-test and one-way analysis of variance (ANOVA) on surfaces machined were carried out. Results for UP insert are included in Fig. 3. The top and bottom corners of the diamonds indicate 95% confidence interval (CI) while the horizontal diagonal indicates the mean grain size. The non-intersecting circles of the Student's *t*-test indicate the grain sizes at low and high speed are statistically different. The grain sizes produced from new and worn inserts at 91 m/min did not show significant difference.